DOI: 10.1021/cg100235x

CRYSTAL
GROWTH
&DESIGN
Article
2010, Vol. 10
2409–2420

Molecular and Supramolecular Diversity Displayed by Dienone-Ether Macrocycles

Luke T. Higham,[†] Janet L. Scott,*[,†] and Christopher R. Strauss*[,‡]

[†]*School of Chemistry and Centre for Green Chemistry, Monash University, Wellington Road, Clayton, Victoria 3800, Australia, and* [‡]*QUILL Centre, The Queen's University of Belfast, David Keir Building, Stranmillis Road, Belfast BT9 5AG, Northern Ireland, U.K.*

Received February 19, 2010; Revised Manuscript Received March 30, 2010

ABSTRACT: Dienone-ether macrocycles (DEMs) represent a new class of supramolecular building blocks for the preparation of crystalline materials with potentially diverse applications. A modular, building block approach to the synthesis employs a range of linked aryl aldehydes and cyclic ketones. Consequently, the structures of DEMs can be tuned with regard to size and shape and the incorporation of functional elements for specific purposes. Fourteen examples are presented, illustrating the diversity of DEMs accessible by this approach. The effect of molecular structure on conformation, supramolecular inclusion, and crystal packing is discussed.

Introduction

Calixarenes,[1] resorcinarenes,[2] cyclotriveratrylenes,[3] cucurbiturils,[4] and crown ethers[5] exemplify families of macrocyclic compounds that have found extensive use in supramolecular chemistry. Key features such as facial curvature and the ability to include or coordinate metal ions have given rise to many and varied applications of such compounds. Recent examples include bowl-shaped cyclotriguaiacylene capsules,[6] resorcinarene cocrystals,[7] calixarene/drug[8] and calixarene/quinoline[9] inclusion complexes, calixarene/metal self-inclusion polymers,[10] and macrocycles bearing crown ether-like moieties.[11]

Such molecules typically are produced from single repeating units. Accordingly, the synthetic strategies in effect afford macrocyclic oligomers. An unfortunate consequence is that they limit the scope for incorporation of structural diversity. If mixtures of starting units were to be employed instead of single components, complex mixtures of essentially randomly generated products could be expected. Pure products could prove difficult to produce in satisfactory yields and to isolate. Consequently, if synthetic modifications were required in order to obtain specific macrocyclic molecules having requisite shape, size, charge distribution, or functional group arrays, the chemistry usually would need to be performed after formation of the macrocyclic ring. In many cases, the identical nature of the various repeated individual units making up the macrocycle would hamper exclusive reaction at a predetermined position on a specific moiety.

We have attempted to avoid these circumstances by developing a versatile array of novel, highly functionalized macrocycles that could be assembled readily from individual building blocks. Efforts have been made to incorporate into the design various means of switching the shape of these molecules to enable them to capture and release specific substrates efficiently and economically. Molecular shape can be altered, for example, by changing the polarity of the solvent and in other cases by exposure to light.[12]

The building block approach[13] employing aryl aldehydes and cyclic ketones delivered a family of molecules referred to herein as dienone-ether macrocycles (DEMs).[14] Such compounds could be transformed in one step to flexible Horning-crowns, for example, a family of macrocycles with structures that are hybrids of calixarenes and crown ethers.[15]

Strategic selection of appropriate salicylaldehyde, dibromo linking units and cycloalkanone reactants enables the size and shape of a DEM to be predetermined and specific functional groups to be inserted (Scheme 1).

Rectangular or parallelogram-shaped (as viewed from above) macrocycles are formed by four sequential Claisen–Schmidt condensation reactions involving two identical linkers. Linkers of differing chain lengths may be inserted by application of the multitasking solvent and catalyst, DIMCARB, as disclosed previously (Scheme 1).[13,16,17] To convey the building block approach and to outline its flexibility, we have used a plumbing analogy. Building blocks bearing activated, nucleophilic methylene groups have been designated as *male*, and those bearing electrophilic, nonenolizable aldehydic functionalities, as *female*.[18] In DEM syntheses, they correspond to cycloalkanone rigid male linkers **II** and salicylaldehyde-based flexible female unions **IV**, as illustrated in Figure 1. Compounds **III**, prepared by DIMCARB mediated condensation, are thus flexible male unions. A vast range of salicylaldehyde and cycloalkanone derived components is available commercially, and dibrominated linkers are readily prepared. Hence, a multitude of DEMs can be produced, and molecular diversity can be readily generated without the need for complex synthetic strategies.

Herein we illustrate both the ease with which these macrocycles may be synthesized and the diversity of shapes and sizes that are accessible. The crystal structures of a range of DEMs are compared to illustrate the effects on the size and shape of variations in structure as well as the impact of structural modification on solid-state packing motifs and intermolecular interactions. The broad scope of molecular and supramolecular structures accessible suggests

---

*To whom correspondence should be addressed. Current addresses: J.L.S.: Centre for Sustainable Chemical Technologies, University of Bath, Bath BA2 7AY, U.K.; e-mail, j.l.scott@bath.ac.uk; telephone, +44 1225 386073. C.R.S.: Strauss Consulting Ltd, P.O. Box 1065, Kunyung LPO, Mt Eliza, Victoria 3930, Australia.

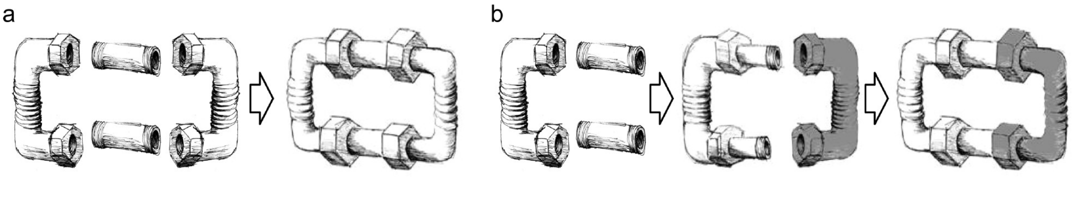

Figure 1. Schematic of construction of (a) a “symmetrical” DEM with identical flexible linkers from two flexible female unions and two rigid male unions, and (b) an “unsymmetrical” DEM with different flexible linkers prepared by sequential assembly of a flexible male union from a flexible female union and two rigid male unions, followed by reaction with a second (different) flexible female union.

Scheme 1. Synthetic Route to DEMs[a]

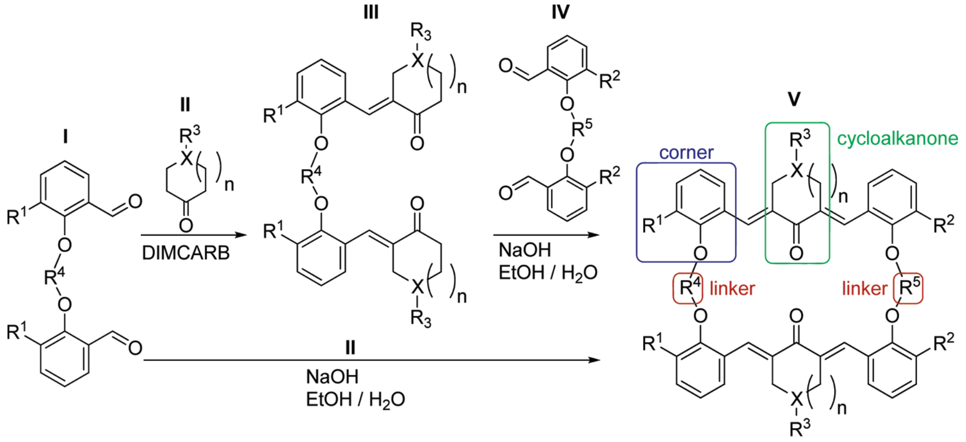

[a] Aryldialdehyde flexible female unions **I** are prepared from salicylaldehydes and dibromo linkers by microwave-assisted Williamson etherification in EtOH; reaction with a cycloalkanone **II** in DIMCARB yields a flexible male union **III**, which may in turn be reacted with a second flexible female union **IV** in a Claisen−Schmidt condensation to afford the DEM **V**. If $R^4 = R^5$, direct reaction of flexible female union **I** with the cycloalkanone in a Claisen−Schmidt condensation reaction provides access to a “symmetrical” DEM.

Table 1. DEMs Reported in This Work

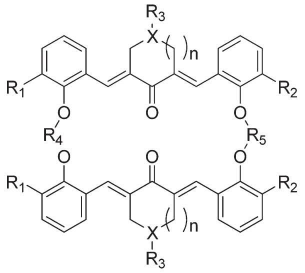

no.	R^1	R^2	R^3	R^4	R^5	X	*n*	yield[a]/%	crystal structure
1	H	H	H	$(CH_2)_2$	$(CH_2)_2$	CH	0	39	CH_2Cl_2 solvate
2	OMe	OMe	H	$(CH_2)_2$	$(CH_2)_2$	CH	0	32	CH_2Cl_2 solvate
3	OEt	OEt	H	$(CH_2)_2$	$(CH_2)_2$	CH	0	21	
4	H	H	H	$(CH_2)_2$	$(CH_2)_2$	CH	1	34[14]	CH_2Cl_2/CH_3CN solvate[14]
5	H	H	Me	$(CH_2)_2$	$(CH_2)_2$	CH	1	39	(*s*,*s*)-isomer chlorobenzene solvate
6	H	H	*t*-Bu	$(CH_2)_2$	$(CH_2)_2$	CH	1	31	(*s*,*s*)-isomer *p*-xylene solvate
7	H	H	Ph	$(CH_2)_2$	$(CH_2)_2$	CH	1	28	
8	OMe	OMe	H	$(CH_2)_2$	$(CH_2)_2$	CH	1	25	CH_2Cl_2 solvate
9	OEt	OEt	H	$(CH_2)_2$	$(CH_2)_2$	CH	1	21	nonsolvated
10	H	H	H	$(CH_2)_2$	$(CH_2)_3$	CH	1	24[13]	$CHCl_3/H_2O$ solvate[13]
11	H	H	H	$(CH_2)_2$	$(CH_2)_2O(CH_2)_2$	CH	1	22[13]	*p*-xylene/water solvate
12	H	H	H	$(CH_2)_2O(CH_2)_2$	$(CH_2)_2O(CH_2)_2$	CH	1	25[14]	
13	H	H	Me	$(CH_2)_2$	$(CH_2)_2$	N	1	31	CH_2Cl_2/toluene solvate
14	H	H	H	$(CH_2)_4$	$(CH_2)_4$	CH	1	18	

[a] Yields are for recrystallized material, with typically narrow melting point ranges (NMR spectra are provided in the Supporting Information) and are based on dialdehyde **I**.

that the potential applications of DEMs (and the related Horning-crowns that may be derived therefrom[15]) may become as wide as those of calixarenes, resorcinarenes, or crown ethers, particularly for the preparation of crystalline materials.

Results and Discussion

The DEMs prepared and described herein are summarized in Table 1. They include examples with linkers of various lengths and composition, *para*-substituted cycloalkanone

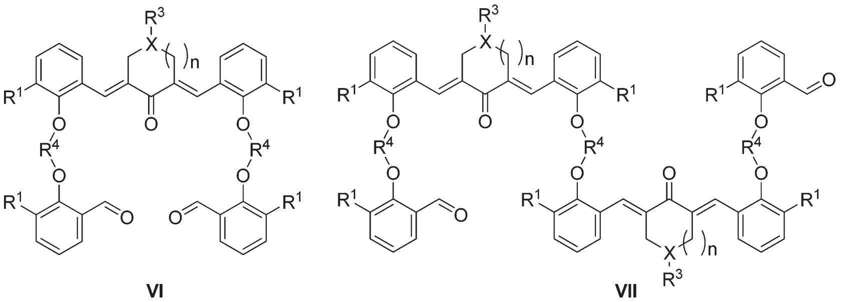

VI VII

Figure 2. Compounds **VI** and **VII**.

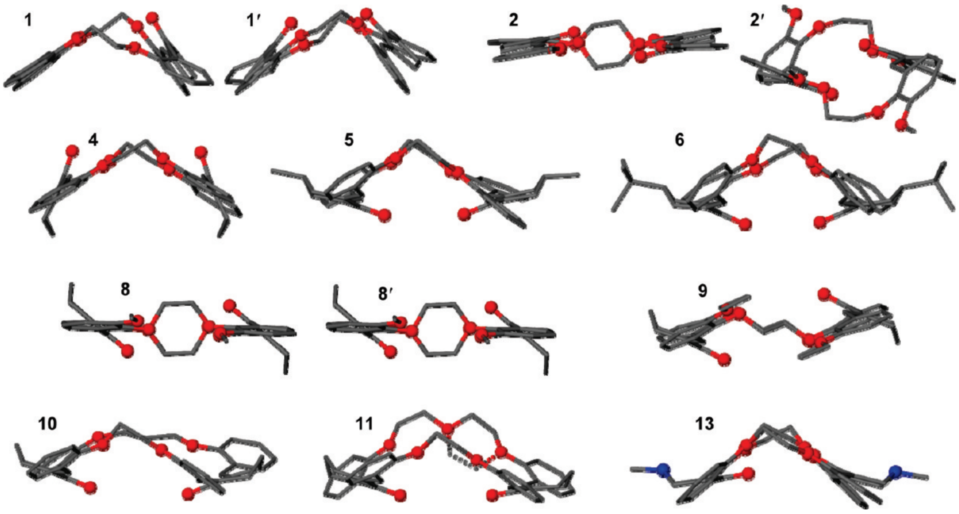

Figure 3. Side views of macrocycles showing the shape adopted in each of the crystal structures. Crystal structures of **4** and **10**, previously published,[13,14] are included for comparison. In all cases the view is oriented such that the C=O group labeled O1 or O1′ is to the left and oxygen and nitrogen atoms are represented as spheres with all other atoms rendered in stick mode. (The second disorder component in **11** is depicted with dashed bonds; in all other cases only the major components are shown.)

moieties, and aryl corners bearing differing substituents. An example of a heteroatom-containing cycloalkanone moiety is also provided.

Although yields were not high, all synthetic steps were executed without protection/deprotection or preactivation strategies, and tandem or cascade-type processes were employed where possible to minimize sequences (Scheme 1). Dilute conditions afforded the DEM as the major product. In general, cyclopentanone reacted more rapidly than did cyclohexanone in the condensations performed, and product DEMs tended to precipitate from solution. ^{1}H NMR spectra of DEMs derived from 4-substituted cyclohexanones exhibited signals due to two distinct species, designated "(*s*,*s*)" or "(*s*,*r*)" with respect to the orientation of the *para* substituents of the cyclohexanone moiety. Also, ^{1}H and ^{13}C NMR spectra of DEMs were sometimes complicated by additional signals attributable to conformers arising from *E*/*Z* photoisomerism of double bonds. The thermodynamically preferred *E*,*E*,*E*,*E* conformers are formed exclusively in Claisen condensations and could be isolated in all cases. Mixed *E*,*Z* conformers may be formed subsequently. They were isolated by selective crystallization, and the photoisomerism of these macrocycles will be reported elsewhere. Byproducts, including "deletion products", i.e. those lacking one cycloalkanone male union, such as **VI** (see Figure 2), or short oligomers, such as **VII**, could be difficult to separate from the desired DEM. This resulted in product losses during purification by recrystallization. The primary focus of this work concerns structural diversity rather than optimization of a specific synthesis, and accordingly, the simplicity and flexibility of the synthetic route makes it amenable to parallel synthesis of libraries of DEMs, useful for screening of specific applications as materials.

Indeed, even a relatively small library of < 20 DEMs has allowed us to demonstrate that subtle changes in the DEM molecular structures can significantly influence physicochemical properties. For example, addition of alkoxy groups to the salicylyl corner groups as in **2**, **3**, **8**, and **9** yielded DEMs with significantly greater solubility than that of the unsubstituted parent macrocycles **1** and **4** in a range of common solvents. The ease with which specific functional units may be incorporated by choice of building block suggests potential for applications where specific functionality is required either for direct activity or after further structural elaboration.

To examine the effect of variation of molecular structure on the solid-state structures and conformational arrangements of the DEMs, crystal structures of a range of solvates and nonsolvated forms were examined. For comparison, structures reported previously[13,14]—the dichloromethane/acetonitrile solvate of rectangular DEM **4**[14] and the water/dichloromethane solvate of trapezoidal DEM **10**[13]—are also discussed. ORTEP diagrams with full molecular numbering are provided in the Supporting Information.

In projection, the DEMs approximate a rectangular or trapezoidal shape, but when viewed from side-on, they resemble two semirigid "leaves" linked by flexible ether "hinges."

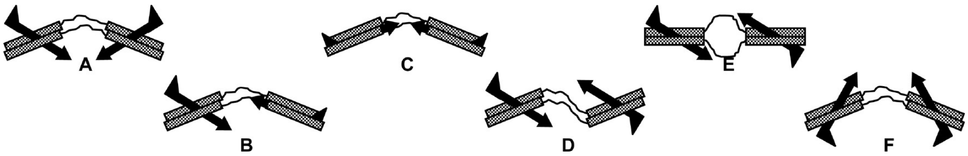

Figure 4. Simplified cartoon depiction of the macrocycle shapes: speckled rectangles represent aryl corner groups (salicylyl moieties), thin lines represent flexible linkers, and arrows represent cyclopentyl or cyclohexyl moieties (with the tail indicating the orientation of the out-of-plane CH_2 group in the envelope conformers of cyclohexyl moieties).

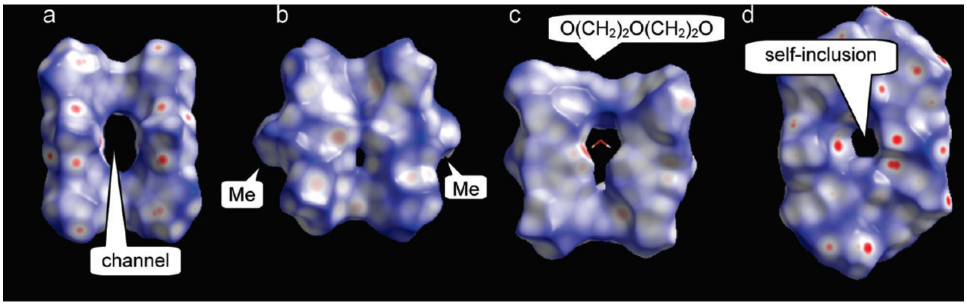

Figure 5. Molecular shape as defined by the Hirshfeld surfaces[19] for the DEMs in (a) **4**; (b) (*s,s*)-**5**; (c) **11** (the hydrogen bonded water molecule is depicted in stick mode); and (d) **9**. All molecules are orientated with bis(benzylidene)cyclohexanone leaves forming the sides, viewed in the hollow of the V (where appropriate) with C═O groups pointing inward.

This conformation allows the bis(benzylidene)cyclohexanone systems to fold relative to each other. Side views of the DEMs show the range of folded structures adopted (Figures 3 and 4). Clearly, even chemically identical macrocycles may adopt various folded or stepped conformations, as occurs in the dichloromethane solvate of **2**.

The relative orientations of the aryl and cycloalkanone moieties may be divided into six types, as depicted in Figure 4. These are characterized, at the extremes, by carbonyl groups swung into the V shape of the folded DEM (form A) and two carbonyl groups reversed out of the cavity (form F). In between these extremes are the following: B, one carbonyl approximately coplanar with the aryl groups; C, both carbonyl groups in-plane with the aryl groups of their respective benzylidene systems; D, carbonyl groups twisted with respect to the approximately coplanar aryl groups but parallel with each other, with aryl groups offset and parallel to each other; and E, as per C, but with approximately coplanar aryl groups (Figure 4). Clearly, these types represent points on a continuum and some macrocycles adopt conformations that are part-way between two types. Thus, type A is found in **5**, **6**, **10**, and **11**; type B in **13**; type C in **1** and **1′** (albeit distorted); type D in **9**; type E in **8** and **8′**; type E in **2** (but not **2′**); and type F in the previously reported **4** only. (Macrocycle **2′** exhibits a remarkably twisted and distorted shape, and we return to discussion of this later.) Clearly, certain types will follow from specific crystallographic symmetry elements; thus, A, C, and F may result when a macrocycle is situated across a mirror plane or centered on a 2-fold axis; D and E may correspond to a center of inversion in the center of the annulus, and B requires that the ASU contains an entire crystallographically unique macrocycle.

The effect of rotation of the carbonyl group out of the hollow of the V of the folded DEM, as in **4**, into the hollow, as in (*s,s*)-**5**, (*s,s*)-**6**, **10**, and **11**, or partially into the hollow, as in **13**, has a dramatic effect on the size of the annulus and the shape of the DEM. Consideration of the shape of the DEMs as their Hirshfeld surfaces, thus illustrating the shape of the molecule *in the crystal* as defined by the "portion of space where the *promolecule* electron density contributes more than half of the total *procrystal* electron density",[19] provides a visual comparison (Figure 5). Conformer type F, represented by **4**, has an open channel through the center of the macrocycle into which solvent molecules pack (Figure 5a), while conformer type A, represented by (*s,s*)-**5**, has no channel. Extension of the length of the flexible linker(s) allows an opening in the center of the DEM, even when the A type conformer is adopted, as is illustrated for **11** in Figure 5c. As a water molecule is hydrogen-bonded across the two C═O groups in **11** in a bridging fashion, the annulus is effectively propped open and this may point to opportunities for inclusion of other hydrogen bond donors into the cavity. The parallel offset conformer D, represented by **9**, exhibits a small hole through the center of the DEM (Figure 5c), which is now flat and extended in length due to the addition of bulky ethoxyl groups to the corner salicylyl moieties (Figure 5d). DEM **9** is the only nonsolvated form, and here the central hole is filled by the ethoxyl group of a neighboring DEM.

In the schematic of the DEM conformers provided in Figure 4, we have depicted aryl groups as parallel with each other and the planar C−C−C(O)−C−C part of the cycloalkanone moiety as flat and uniformly twisted with respect to the aryl groups. The implication is that the "leaves" of the conjugated Ar—C═C—C(O)—C═C—Ar bis(benzylidene)cyclohexanone system seldom adopt a flat conformation and, in these structures, may be bowed or twisted (or both). Indeed, only one (of four in each structure) of the leaves of macrocycles **1** and **2** and one (of two) of the leaves of **13** adopt a largely coplanar arrangement, as is discernible by close examination of Figure 3. Out-of-plane twists of the approximately planar C−C−C(O)−C−C system of cyclopentyl or cyclohexyl groups appear common, and aryl rings of a bis(benzylidene)cyclohexanone system may be twisted with respect to each other. To describe these twists and bows, the planes and lines depicted in Figure 6 are used to effect measurement of the dihedral angles between aryl rings and an adjacent C−C(O)−C group, ∠1 and ∠2, and between aryl groups of the same leaf, ∠3 (Table 2). The angle between lines coincident with C═O groups of opposite leaves is used to define the pitch of the V.

One bis(benzylidene)cyclohexanone leaf of **1** approaches planarity, as does one leaf of **13** and both leaves of **2** (second generated by symmetry). At the opposite end of the spectrum, both leaves of **2′** are highly twisted, and thus, the independent DEMs in the crystal structure have very different shapes, as is illustrated by comparison of their Hirshfeld surfaces (Figure 7).

To discern whether certain DEM molecular conformations lead to specific solid state packing and/or intermolecular interactions (or vice versa), the crystal structures were compared and grouped. Analysis of the extended packing motifs of the different macrocycles reveals four main types of structure:

1 Overlapped $\pi\pi$ stacked DEM systems.
2 Structures containing channels in which solvent is accommodated.
3 Structures dominated by CH···O═C interactions.
4 Nonsolvated structures in which self-inclusion of a neighboring DEM replaces solvent inclusion.

Classifying the structures in this manner leads to an interesting correlation between conformer type and extended packing motif, illustrated in Table 3. It appears that certain conformer types are correlated with particular extended packing motifs. Conformer types C and B are similar, differing by rotation of one C−C(O)−C group into the V. Thus, both $\pi\pi$ stacked systems adopt similar B and C conformers and two of the three channel type systems adopt the E

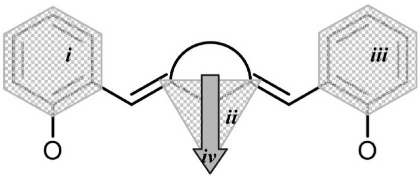

Figure 6. Planes and lines defined to describe the twist and bow of bis(benzylidene)cyclohexanone leaves and the dihedral angle between C═O groups of opposite leaves of the DEMs. Planes *i* and *iii* are the aromatic rings and *ii* the C−C(O)−C system, while line *iv* defines the C═O group.

Table 3. Classification of Structures into Extended Structure Types and DEM Conformer Types

Extended structure	Crystal structure	Conformer type	
$\pi\pi$ stacked systems	**1**•2CH$_2$Cl$_2$	C	
	13•CH$_2$Cl$_2$•toluene	B	
Channels	**2**•CH$_2$Cl$_2$	E	
	4•¾CH$_2$Cl$_2$•½CH$_3$CN	F	
	8•2CH$_2$Cl$_2$	E	
CH···O=C interactions	s,s-**5**•C$_6$H$_5$Cl	A	
	s,s-**6**•1½*p*-xylene	A	
	10•½CHCl$_3$•H$_2$O	A	
	11•*p*-xylene•1½H$_2$O	A	
self inclusion	**9**	D	

Table 2. Molecular Geometry Defined by Relative Angles between Planes and Lines of the Bis(benzylidene)cyclohexanone Moieties and across the Macrocycle

DEM	conformer type	∠1/deg (plane *i* − *ii*)	∠2/deg (plane *ii* − *iii*)	∠3/deg (plane *i* − *iii*)	∠4/deg (line *iv* − *iv*)
1	C	4.1(2)	9.0(2)	9.9(2)	87.6(2)
		7.4(2)	43.3(2)	35.9(2)	
1′	C	11.0(3)	36.9(3)	30.4(3)	80.4(2)
		8.8(3)	31.9(2)	33.6(1)	
2	E	4.3(4)	14.6(3)	10.3(3)	‖[a]
2′	[b]	5.0(2)	69.6(2)	74.5(2)	‖[a]
4	F	42.1(2)	42.6(2)	15.1(2)	36.9(1)[c]
5	A	55.6(1)	62.3(1)	33.2(1)	43.6(1)
		43.1(1)	60.0(1)	17.4(1)	
6	A	57.4(1)	73.7(1)	39.5(1)	49.2(2)
		61.3(2)	68.8(2)	34.3(2)	
8	E	36.9(1)	40.9(1)	13.0(2)	‖[a]
8′	E	36.6(1)	38.5(1)	11.7(2)	‖[a]
9	D	47.2(1)	53.9(1)	23.2(1)	‖[a]
10	A	49.5(1)	56.3(1)	26.8(1)	44.0(1)
		46.2(1)	59.3(1)	38.7(1)	
11	A	49.7(1)	70.5(1)	42.7(1)	30.3(2)
		45.8(1)	49.3(1)	30.1(2)	
13	B	31.3(2)	34.7(2)	14.2(2)	38.5(1)
		6.8(2)	17.5(2)	11.6(1)	

[a] These planes are parallel because the second C═O group is generated by a center of symmetry from half a macrocycle of the ASU. [b] Twisted conformation not categorized. [c] Symmetry transformation operation used to define the opposite cycloalkanone C−C(O)−C motif: $1 - x, y, {}^1/_2 - z$.

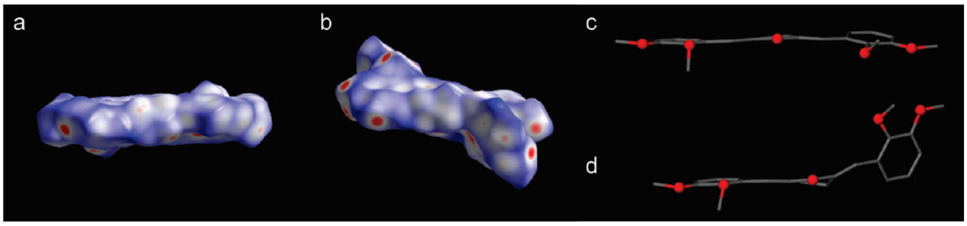

Figure 7. Hirshfeld surfaces of (a) **2** and (b) **2′**. Single leaves viewed down the line OC of the C═O group (c) **2** is almost planar, and (d) **2′** shows the large out of plane twist and bend of one aryl group.

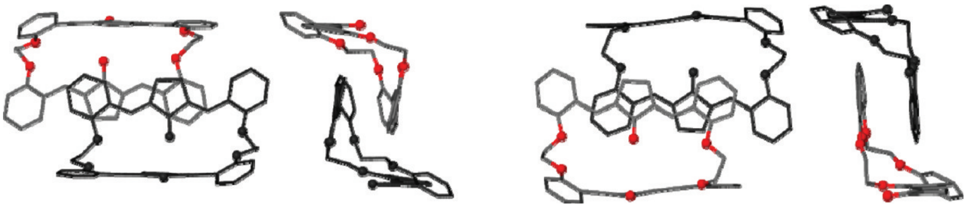

Figure 8. "Face to face" $\pi\pi$ overlap in (a) DEM **1** and (b) DEM **1′** in the **1**·2CH$_2$Cl$_2$ solvate structure with symmetry generated macrocycles depicted in dark gray and oxygen atoms as spheres. Both DEMs are in the C type conformation, but the rings of each leaf are not entirely coplanar. Instead, the overlapped parts tend to adopt a planar arrangement, while the nonoverlapped aryl ring is slightly twisted out of the plane.

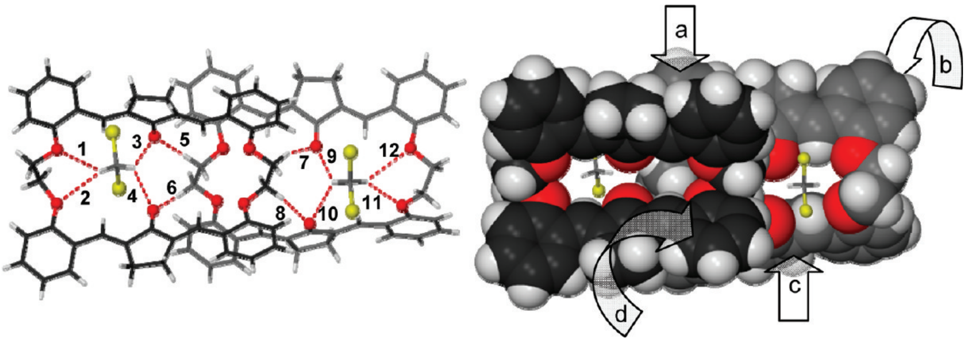

Figure 9. Intermolecular interactions in **1**·2CH$_2$Cl$_2$ (a) illustrated in stick mode with close contacts indicated by dotted lines (**1′** DEM, generated by the symmetry operator $x - 1, 1 + y, z - 1$, is depicted in dark gray) and (b) in space fill mode with arrows indicating the $\pi\pi$ overlap. These are: (a) back to back $\pi\pi$ overlap of **1′**, (b) face to face $\pi\pi$ overlap of **1** (as depicted in Figure 8a), (c) face to face $\pi\pi$ overlap of **1′** (as depicted in Figure 8b), and (d) back to back $\pi\pi$ overlap of **1**.

Table 4. Summary of CH···O Interactions in 1 and 13

		C–H···O^{a}	d(H···A)/Å	d(D···A)/Å	∠DHA/deg
1	1	C3G1–H3G1^{a}···O2′	3.44	4.28(1)	145
	2	C3G1–H3G1^{a}···O3′	3.02	3.97(1)	162
	3	C3G1–H3G2^{a}···O1′	2.49	3.245(6)	133
	4	C3G1–H3G2^{a}···O4′	2.52	3.206(6)	126
	5	C6–H6A^{b}···O1′	2.41	3.317(5)	153
	6	C7–H7A^{b}···O4′	2.52	3.320(5)	138
	7	C18′–H18D^{c}···O1	2.56	3.389(5)	142
	8	C17′–H17D^{c}···O4	2.29	3.213(5)	154
	9	C4G–H4G2···O1	2.39	3.078(5)	126
	10	C4G–H4G2···O4	2.73	3.451(5)	130
	11	C4G–H4G1···O6	2.95	3.809(5)	146
	12	C4G–H4G1···O5	2.53	3.425(5)	150
13	1	C8G–H8G2···O5	3.68	4.337(4)	126
	2	C8G–H8G2···O6	2.79	3.512(4)	130
	3	C8G–H8G1···O4	2.47	2.947(4)	109
	4	C8G–H8G1···O1	2.86	3.192(4)	100

[a] Symmetry operations used to define atoms: (a) $x - 1, y, z$; (b) $x, y - 1, 1 + z$; (c) $x, 1 + y, z - 1$.

conformer. All structures characterized by the CH···O=C interactions have DEMs in the A conformer, which decreases the size of the annulus in the DEM, and the nonsolvate is the only structure wherein the DEM adopts the D conformer. The previously described solvate, **4**·$^{3}/_{4}$CH$_2$Cl$_2$·$^{1}/_{2}$CH$_3$CN, also proves to be an odd structure out, but this will be discussed under the section on channel type structures.

$\pi\pi$ Stacked Systems. In the absence of strong intermolecular interactions, such as hydrogen bonds, a number of weaker interactions may be discerned in a study of close contacts. Thus, in **1**·2CH$_2$Cl$_2$ a series of $\pi\pi$ stacking interactions were noted between DEMs (Figure 8). The "face to face" $\pi\pi$ overlapped systems all adopt a flat or nearly flat conformation, while nonoverlapped aryl groups may be twisted well out of the plane.

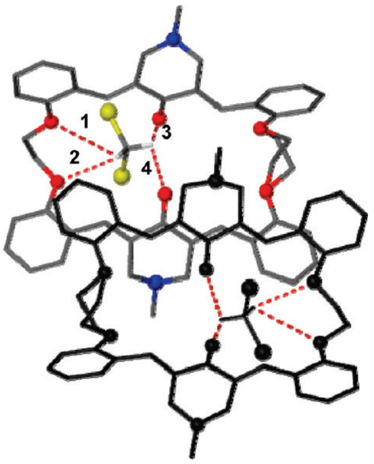

Figure 10. DEM intermolecular interactions in the **13**·CH$_2$Cl$_2$·toluene solvate structure. Oxygen, nitrogen, and chlorine atoms are depicted as spheres and CH···O interactions as dotted lines. Unusually, $\pi\pi$ overlap is not offset and closest distances between planes are atom/atom distances. This "in registration" configuration is usually considered to be energetically unfavorable and one must consider it possible that this is a weakly repulsive interaction *imposed by* packing rather than a weakly attractive interaction *leading to* specific arrangements of molecules.

As illustrated in Figure 9, two included CH$_2$Cl$_2$ solvent molecules exhibit close contacts with the oxygen atoms of the DEM and the solvent molecule is fitted into a cavity on the apex of the V of the DEMs to one side of the C=O groups. The corresponding cavity on the other side is filled by the side chain of the second DEM with corresponding close contacts between methylene hydrogen atoms and carbonyl oxygen atoms (Table 4). The pairs of DEMs so formed then pack in the extended structure such that partial overlap of π systems of adjacent pairs occurs, in either a back-to-back or face-to-face manner (Figure 9).

In **13**, similar insertion of the CH_2Cl_2 solvent into the apex of the V and face to face $\pi\pi$ overlap occurs (Figure 10), but the CH···O interactions of one ethereal linker of one DEM with the carbonyl groups of its neighbor (that resulted in a "clipping together" of the DEMs) are lacking, as are back to back $\pi\pi$ interactions. CH···O distances (summarized in Table 4) are longer and an unusual "in registration" arrangement of the overlapped unsaturated systems occurs (Figure 10).

The extra solvent molecules, $2CH_2Cl_2$ and toluene, in **1** and **13**, respectively, appear to fill cavities in the structure, and an isomorphous solvate structure of **13**·CH_2Cl_2·EtOAc, where a molecule of ethyl acetate adopts the position of toluene, has also been isolated (not reported here).

Channels. The two conformational types leading to channel type structures are quite different: E results from parallel offset C=O groups, while F results from C=O groups rotated out of the hollow of the V shaped DEM. In both cases, however, a central cavity is opened up and solvent molecules may be accommodated in this space. Packing diagrams of both E type conformer structures are presented in Figure 11.

The packing diagram of **2**·CH_2Cl_2 (Figure 11a) is particularly revealing, as it becomes clear that the previously nonclassifiable, twisted conformer **2′** is not part of the channel forming structure but serves to fill space, separating sheets of parallel channels and propping the almost flat DEMs **2** apart to accommodate the solvent molecules. The two independent DEMs **8** and **8′** (two and a half DEMs in the ASU) both adopt the open annulus shape in the **8**·$2CH_2Cl_2$

Table 5. Summary of CH···O Interactions in 2 and 8

		C−H···O	*d*(H···A)/Å	*d*(D···A)/Å	∠DHA/deg
2	1	C1G−H1GB···O1	2.65	3.513(7)	146
8	1	C1G−H1G′···O1	2.29	3.125(4)	142
	2	C2G−H2G···O1′	2.30	3.124(4)	141

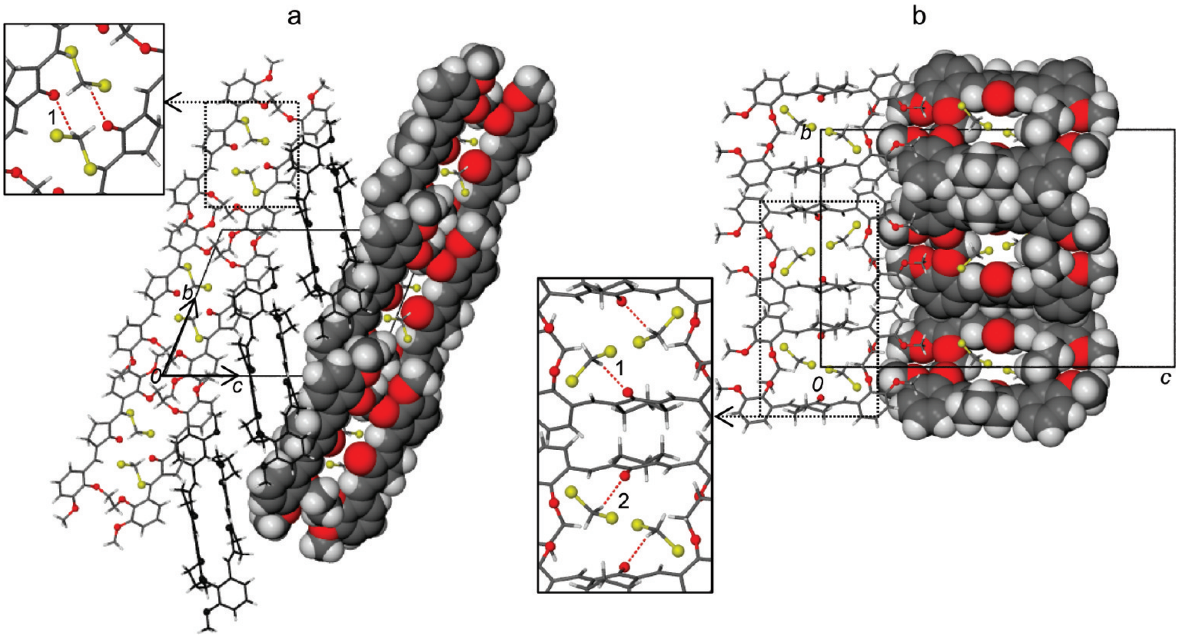

Figure 11. Packing diagrams of (a) **2**·CH_2Cl_2 and (b) **8**·$2CH_2Cl_2$, both viewed down [1 0 0]. In part a, channels formed by **2** and accommodating CH_2Cl_2 molecules are clearly visible, while **2′**, depicted in dark gray, does not participate in channel formation. In part b, both DEMs (two and a half DEMs in the ASU) form channels. Close CH···O contacts between CH_2Cl_2 molecules and C=O groups are shown in the insets.

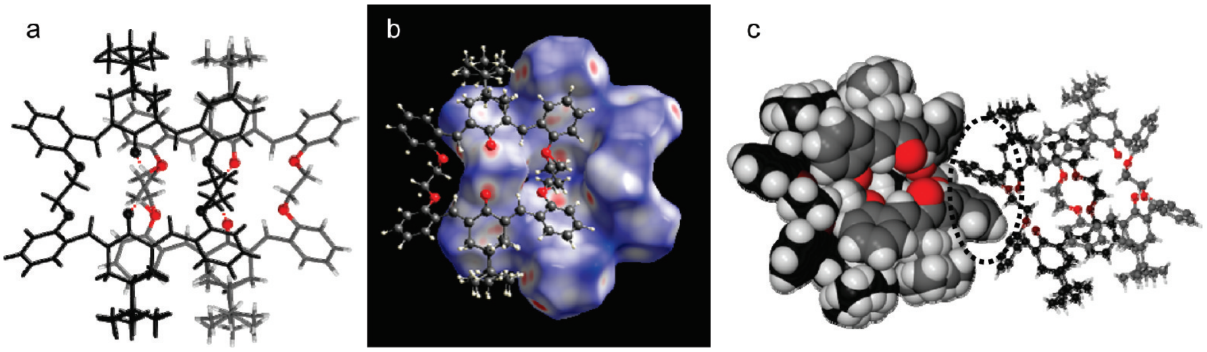

Figure 12. (a) Overlapping DEMs in (*s,s*)-**6**·$1^1/_2$*p*-xylene. One DEM is illustrated with CPK coloring, while the second symmetry generated DEM is depicted in dark gray. CH···O close contacts are indicated with dotted lines, and all disordered groups are shown. Note that flexible linker disorder results in alternate C−H···O interactions between CH_2 and C=O groups. (b) Overlapping DEMs with one molecule depicted as its Hirshfeld surface. The bulge due to flexible linker puckering fits into the cavity of the neighboring macrocycle. (c) Pairs of DEMs overlapped as illustrated in parts a and b exhibit $\pi\pi$ stacking with neighboring pairs.

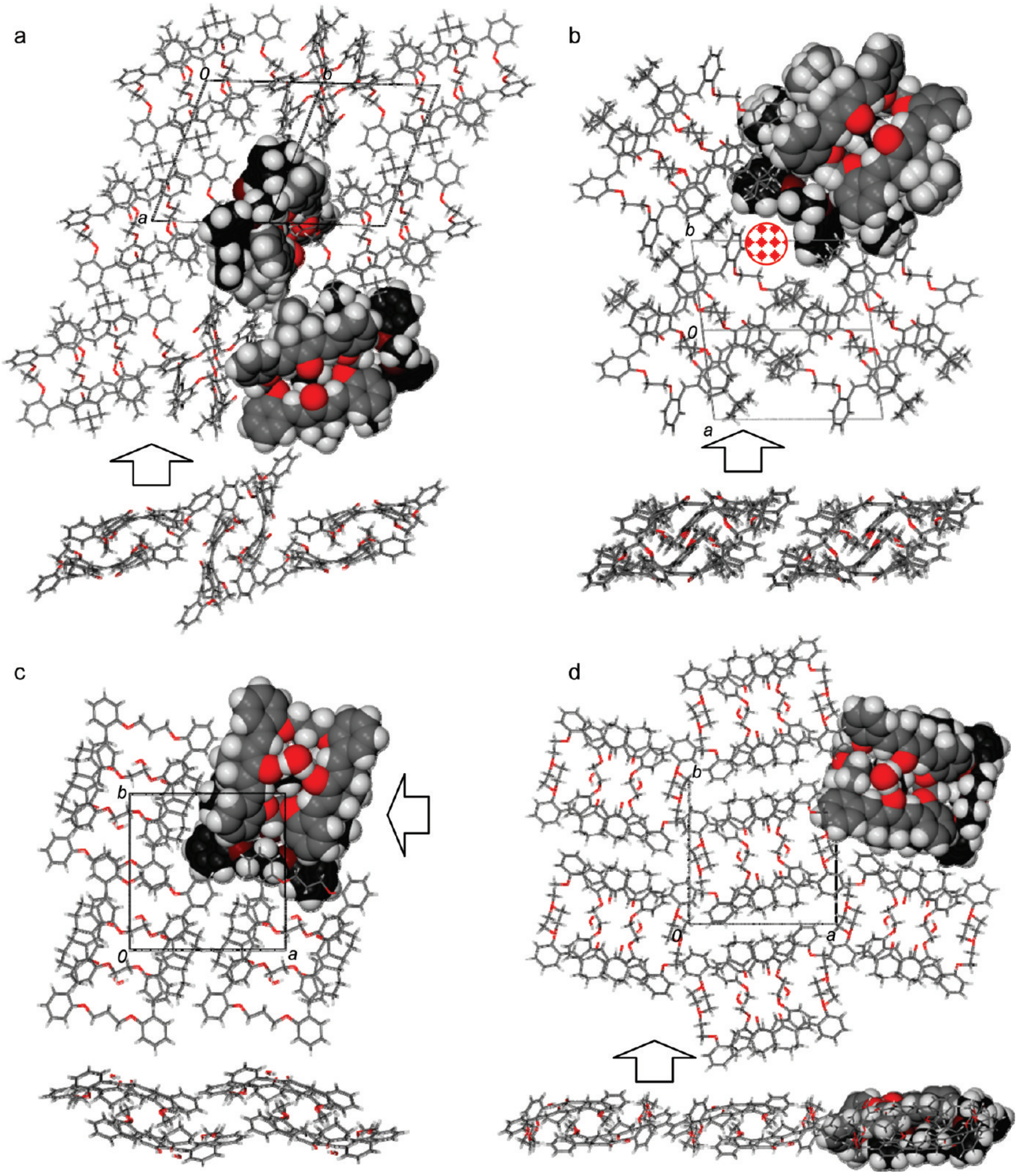

Figure 13. Packing diagrams of (a) (s,s)-**5**$\cdot C_6H_5Cl$ viewed down [0 1 −1] (top) and rotated; (b) (s,s)-**6**$\cdot 1^1/_2$*p*-xylene viewed down [1 1 0] and rotated; (c) **10**$\cdot {}^1/_2CHCl_3\cdot H_2O$ viewed down [0 0 −1] and rotated; (d) **11**$\cdot$*p*-xylene$\cdot 1^1/_2H_2O$ viewed down [0 0 1] and rotated. In all cases included, solvent molecules have been removed for clarity (except the strongly hydrogen bonded water molecules in parts c and d), and one or two pairs of DEMs are depicted in space filling mode with an arrow to indicate the direction of view of the rotated layer below each packing diagram. The DEMs depicted in parts b, c, and d tend to form puckered sheets, and only one sheet is depicted in each case—the subsequent layer is offset such that hollows and humps are suitably aligned. Conversely, (s,s)-**5** (in the structure of the chlorobenzene solvate) (a) does not form puckered sheetlike structures of similarly orientated DEMs but has alternating rows of pairs forming sheets of variable thickness. Solvent molecules fill spaces left by imperfect packing or even fill cavities in sheets, as in part b, where the hatched circle demarcates a solvent position.

solvate (Figure 11b). Describing these as channel forming may be a little misleading, as the channel walls result from intercalation of side chains (**8**$\cdot 2CH_2Cl_2$) or rings and side chains (**2**$\cdot CH_2Cl_2$), *and* the open annulus forming conformation of the DEM. In common with other CH_2Cl_2 solvates, close contacts between solvent hydrogen atoms and DEM oxygen atoms are noted, as depicted in the inset close-ups in Figure 11 and listed in Table 5.

These two conformer type E channel structures differ from that of **4** in the F conformer previously published,[14] where the channel walls are largely due to the truncated conelike shape of the DEM resulting from twisting of the C=O groups out of the hollow of the V and true cavity inclusion occurs. The constricted channels of **8** are reflected in a relatively high guest loss temperature, as measured by thermogravimetric analysis, where DCM solvent is lost in the range 80−120 °C. This is reflected in the stability of this complex, with single crystals of **8**$\cdot 2CH_2Cl_2$ showing no loss of crystallinity when exposed to the atmosphere for a lengthy period.

CH···O=C interactions. The most commonly encountered conformer type in these DEM solvate crystals is the A type, where both carbonyl groups are rotated into the hollow of the V of the folded DEM. In all cases, these DEMs pack together in pairs with a side chain of one protruding into the hollow of its neighbor, as is illustrated for the (s,s)-isomer of

6 in the *p*-xylene solvate (Figure 12). This results in hydrogen atoms of flexible linker methylene groups coming into relatively close contact with DEM carbonyl group oxygen atoms.

This motif of overlapped complementarily shaped DEMs in the **A** type conformer with CH$\cdots$O=C close contacts is repeated in (s,s)-**5**·C_6H_5Cl, **10**·$^1/_2CHCl_3\cdot H_2O$, and **11**·*p*-xylene·$1^1/_2H_2O$, but the interactions and relative orientations of neighboring pairs of DEMs differ markedly from structure to structure, as is illustrated in the partial packing diagrams (Figure 13). A summary of CH$\cdots$O close contacts is provided in Table 6. Clearly, the differing shapes of the DEMs provide (or frustrate) opportunities for a series of CH$\cdots$O interactions both with oxygen atoms of the carbonyl groups (used to categorize this group of structures) and of the ethereal flexible linkers. In some cases, packing of neighboring sheets or pairs of DEMs is such that further CH$\cdots$O close contacts are possible (Table 6), indicating the possible importance of this relatively weakly attractive interaction in the absence of other stronger interactions, such as traditional hydrogen bonds. The C−H$\cdots$O=C supramolecular synthon may reflect either classical, weak CH$\cdots$O hydrogen bonding or the less oft discussed electrostatic interaction between somewhat acidic protons and π systems, i.e. C−H$\cdots\pi$(O=C).[20] We have tended to focus on the former as a defining interaction in this group of structures, but it is certain that there is also an element of the latter in many cases.

Table 6. Summary of CH$\cdots$O Interactions in (s,s)-5, (s,s)-6, 10, and 11

	C−H$\cdots$O^a	d(H$\cdots$A)/Å	d(D$\cdots$A)/Å	∠DHA/deg
5	C18−H18B$^a\cdots$O4	2.43	3.253(3)	140
	C18−H18A$^a\cdots$O6	2.64	3.253(3)	142
	C40−H40$^a\cdots$O2	2.66	3.574(3)	163
	C29−H29$^b\cdots$O1	2.34	3.236(3)	158
6	C7−H7A$^c\cdots$O1	2.58	3.380(6)	138
	C7−H7B$^c\cdots$O3	2.75	3.632(7)	149
	C29−H29$^c\cdots$O5	2.71	3.589(5)	154
	C30−H30$^c\cdots$O6	2.52	3.403(5)	154
10	C6−H6A$^d\cdots$O4	2.55	3.440(3)	150
	C7−H7A$^d\cdots$O1	2.65	3.465(3)	140
	C18−H18B$\cdots$O7	2.80	3.700(4)	152
	C19−H19B$^e\cdots$O1	2.68	3.672(3)	178
	C27−H27$^f\cdots$O7	2.44	3.281(3)	147
	C31−H31$^d\cdots$O6	2.65	3.426(3)	140
	C43−H43$^e\cdots$O4	2.84	3.764(3)	165
11	C6−H6B$^g\cdots$O2	2.60	3.465(5)	146
	C6−H6A$^g\cdots$O4	2.36	3.251(5)	150
	C6−H6A$^g\cdots$O1W	2.78	3.581(5)	138
	C7−H7A$^g\cdots$O1	2.66	3.402(5)	132
	C17−H6C$^h\cdots$O6	2.64	3.47(1)	142
	C18−H18D$^h\cdots$O5	2.31	3.27(1)	164
	C30−H30$^g\cdots$O5	2.63	3.382(5)	136

[a] Symmetry operations used to define atoms: (a) $-x$, $1 - y$, $1 - z$; (b) x, $^1/_2 - y$, $z - {}^1/_2$; (c) $1 - x$, $1 - y$, $-z$; (d) $2 - x$, $-y$, $-z$; (e) $2^1/_2 - x$, $y - {}^1/_2$, $^1/_2 - z$; (f) $2^1/_2 - x$, $^1/_2 + y$, $^1/_2 - z$; (g) $1 - x$, $3 - y$, $-z - 1$; (h) $-x$, $3 - y$, $-z - 1$.

It is notable that the hydrate forms, **10**·$^1/_2CHCl_3\cdot H_2O$ and **11**·*p*-xylene·$1^1/_2H_2O$, both adopt the A conformer, form dimers with CH$\cdots$O=C close contacts, and pack in puckered sheetlike structures. In the solid state, the bridging water molecule serves to lock the DEM into the A conformer and one might expect some evidence of dimerization in solutions containing small quantities of water, similar to that detected in the Horning-crown macrocycles derived from these DEMs.[21] In this regard, it is noteworthy that the "(s,s)" and "(s,r)" forms are readily distinguishable by analysis of ^{1}H NMR spectra, which may be indicative that solid state conformers are propagated in solution.

Self-inclusion. The "odd one out" in this collection of structurally diverse, yet related, DEM structures is that of the nonsolvated **9**. Not only is solvent not trapped in the structure, but the DEM adopts a conformation not seen in any of the other examples, that of the parallel offset C=O groups and parallel offset aryl rings, type D.

The extended, flexible ethoxyl substituents of the DEM corner groups become self-included into the annulus of a neighboring macrocycle, thus forming interlocking sheets of DEMs that pack together efficiently without inclusion of space filling solvent molecules (Figure 14).

Conclusions

The modular building-block approach to the synthesis of dienone-ether macrocycles provides simple, direct synthetic access to a range of macrocyclic structures. The ease with which components may be altered to provide materials bearing substituents on any of the ring components or with various linker lengths makes the task of designing a DEM for a particular application a simple task. In addition, numerous commercially available starting materials are available for this

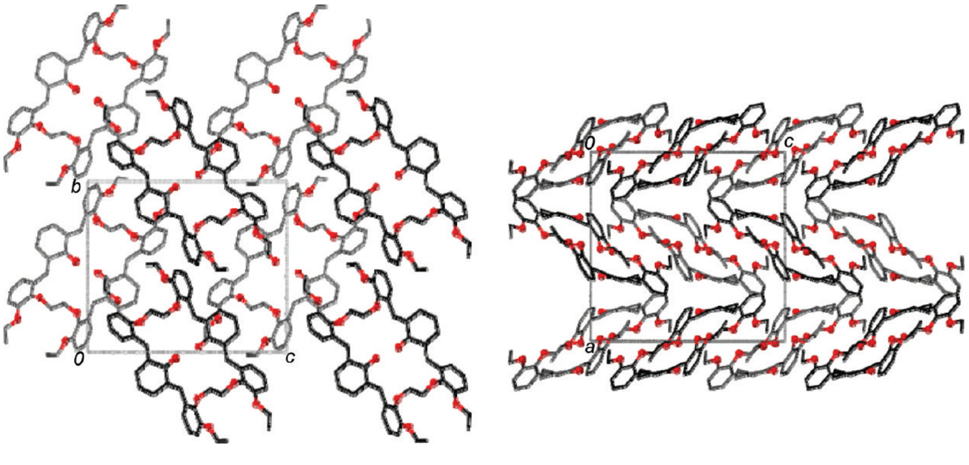

Figure 14. Packing diagrams of **9** viewed down [1 0 0] (left) and [0 1 0] (right). Only one layer is shown at left, but at right, the stacking of layers is depicted. For clarity, alternate DEMs are picked out in darker shades, but note that all molecules are symmetry related and that the ASU contains half a DEM only.

synthetic protocol, allowing tuning of the molecular structure or exploration of molecular space by combinatorial array techniques.

The supramolecular versatility of these materials has also been demonstrated, and this, combined with the relative simplicity and potential greenness of the synthetic method, renders these DEMs appropriate starting materials for the supramolecular, "bottom-up" approach to the development of new crystalline materials. The terms "design" or "designer" have been widely applied to describe macrocycles with variable shapes, sizes, or functional groups that are readily altered either during synthesis or by post synthetic modification. This work indicates that DEMs are equally, if not more, amenable to genuine design for function. Significantly, these macrocycles are complementary to the well-known calixarene, resorcinarene, and crown ether groups that have been investigated actively for decades in that regard.

In addition, as we have described previously,[15] all of these DEMs are readily converted into Horning-crowns: flexible, phenol-ether macrocycles with demonstrated flexibility and switchability, so extending the range of supramolecular building blocks or ligands available for the preparation of crystalline materials.

Experimental Section

Synthesis. The syntheses of DEMs **4**, **10**, **11**, and **12** have been previously reported, and full characterization data are contained in refs 12 and 13. Synthesis of macrocycle **2** is provided as a representative example of all DEM syntheses; detailed syntheses of other DEMs can be found in the Supporting Information. Characterization data of all new DEMs is reported below.

2: (1*E*,11*E*,15*E*,25*E*)-3,4:9,10:17,18:23,24-Tetra(6-methoxybenzo)-5,8,19,22-tetraoxatricyclo[24.2.1.1^{12,15}]triaconta-1,3,9,11,15,17,23,25-octaene-29,30-dione. A mixture of 2,2′-(ethane-1,2-diylbis(oxy))-bis(3-methoxybenzaldehyde) (0.782 g, 2.37 mmol) and cyclopentanone (0.299 g, 3.55 mmol) in 96% EtOH (120 mL) and 20% w/v aq NaOH (3.6 mL, 18 mmol) was stirred at rt for 3 days. The orange solid that had precipitated was collected by vacuum filtration, washed with 1.0 M HCl (2 × 5 mL), water (2 × 5 mL) and 96% EtOH (2 × 5 mL), and dried under vacuum (0.728 g). The solid was recrystallized from CH_2Cl_2 (40 mL) to give the dienone macrocycle **2** (0.283 g, 0.374 mmol, 32%) as a yellow solid; mp 296−298 °C. Anal. Found: C, 72.7; H, 5.7. Calcd for $C_{46}H_{44}O_{10}$: C, 73.0; H, 5.9. δ_H (300 MHz; $CDCl_3$) 7.87 (4 H, s, CH), 7.14 (4 H, dd, *J* 7.9 and 1.4, Ar), 7.06 (4 H, dd, *J* 8.1 and 7.9, Ar), 6.92 (4 H, dd, *J* 8.1 and 1.4, Ar), 4.31 (8 H, s, OCH_2), 3.88 (12 H, s, OCH_3), 2.99 (8 H, s, CCH_2); δ_C (100 MHz; $CDCl_3$) 195.7, 153.0, 148.4, 139.5, 131.0, 128.2, 123.8, 122.2, 113.5, 72.6, 52.2, 26.9; *m*/*z* (ESI) 779.4 (M + Na$^+$, 100%), 757.5 (M + H$^+$, 93).

1: (1*E*,11*E*,15*E*,25*E*)-3,4:9,10:17,18:23,24-Tetrabenzo-5,8,19,22-tetraoxatricyclo[24.2.1.1^{12,15}]triaconta-1,3,9,11,15,17,23,25-octaene-29,30-dione. Yellow solid; mp (dec.) 230 °C; ν_{max}/cm^{-1} (neat) 1687w (C═O), 1617m (olefinic C═C); δ_H (300 MHz; $CDCl_3$) 7.88 (4 H, s, CH), 7.51−7.47 (4 H, m, Ar), 7.34−7.24 (4 H, m, Ar), 7.01−6.89 (4 H, m, Ar), 4.45 (8 H, s, OCH_2), 2.95 (8 H, s, CCH_2); δ_C (75 MHz; CF_3COOD) 200.7, 161.9, 142.9, 138.2, 137.9, 133.9, 126.9, 124.5, 115.3, 69.1, 29.5; *m*/*z* (ESI) 659.3 (M + Na$^+$, 100%); *m*/*z* (ESI) 659.2415 (M + Na$^+$, 100%; $C_{42}H_{36}NaO_6^+$ requires 659.2398).

3: (1*E*,11*E*,15*E*,25*E*)-3,4:9,10:17,18:23,24-Tetra(6-ethoxybenzo)-5,8,19,22-tetraoxatricyclo[24.2.1.1^{12,15}]triaconta-1,3,9,11,15,17,23,25-octaene-29,30-dione. Yellow solid; mp 257−258 °C; ν_{max}/cm^{-1} (neat) 1692w (C═O), 1608m (olefinic C═C); δ_H (300 MHz; $CDCl_3$) 7.91 (4 H, s, CH), 7.15 (4 H, dd, *J* 7.9 and 1.4, Ar), 7.04 (4 H, dd, *J* 8.1 and 7.9, Ar), 6.90 (4 H, dd, *J* 8.1 and 1.4, Ar), 4.35 (8 H, s, OCH_2), 4.08 (8 H, q, *J* 7.0, OCH_2CH_3), 3.01 (8 H, s, CCH_2), 1.47 (12 H, t, *J* 7.0, CH_3); δ_C (100 MHz; CF_3COOD) 195.0, 145.7, 144.4, 133.7 (2C), 131.9, 123.1, 119.4, 117.0, 70.1, 59.6, 21.2, 7.6; *m*/*z* (ESI) 835.3 (M + Na$^+$, 100%); *m*/*z* (ESI) 813.3624 (M + H$^+$, 100%; $C_{50}H_{53}O_{10}^+$ requires 813.3679).

5: (14*S*,29*S*)/(14*S*,29*R*) Isomeric Mixture of (1*E*,11*E*,16*E*,26*E*)-3,4:9,10:18,19:24,25-Tetrabenzo-14,29-dimethyl-5,8,20,23-tetraoxatricyclo[25.3.1.1^{12,16}]dotriaconta-1,3,9,11,16,18,24,26-octaene-31,32-dione. Orange solid; mp 295−296 °C; ν_{max}/cm^{-1} (neat) 1665w (C═O), 1596m (olefinic C═C); δ_H (400 MHz; CF_3COOD) 9.10 and 9.04 (1.00:0.16; 4H, s, CH), 7.71−7.60 (16 H, m, Ar), 7.25−7.18 (16 H, m, Ar), 4.74 (16 H, m, OCH_2), 3.31−3.25 (8 H, m, CH_2), 2.70−2.56 (8 H, m, CH_2), 2.17−1.98 (4 H, m, CH), 1.24−1.20 (12 H, m, CH_3); δ_C (100 MHz; CF_3COOD) 198.1, 197.3, 160.3, 160.1, 146.9, 146.6, 136.5, 136.3, 136.1, 136.0, 133.7 (2C), 127.0, 126.9, 124.0, 123.9, 115.3, 115.0, 68.9, 68.5, 37.9, 37.1, 31.8, 31.0, 21.8, 21.4; *m*/*z* (ESI) 715.3025 (M + Na$^+$, 100%; $C_{46}H_{44}NaO_6^+$ requires 715.3036).

6: (14*S*,29*S*)/(14*S*,29*R*) Isomeric Mixture of (1*E*,11*E*,16*E*,26*E*)-3,4:9,10:18,19:24,25-Tetrabenzo-14,29-di-*tert*-butyl-5,8,20,23-tetraoxatricyclo[25.3.1.1^{12,16}]dotriaconta-1,3,9,11,16,18,24,26-octaene-31,32-dione. Yellow solid; mp 297−298 °C; ν_{max}/cm^{-1} (neat) 1670w (C═O), 1596s (olefinic C═C); δ_H (400 MHz; CF_3COOD) 8.94 (8.86) (4 H, s, CH), 7.66−7.53 (16 H, m, Ar), 7.20−7.11 (16 H, m, Ar), 4.64 (16 H, m, OCH_2), 3.30−3.23 (8 H, m, CH_2), 2.53−2.44 (8 H, m, CH_2), 1.59−1.52 (4 H, m, CH), 0.94−0.93 (18 H, m, CH_3); δ_C (100 MHz; CF_3COOD) 198.8, 197.6, 160.6, 160.4, 146.5 (2C), 146.5, 137.2, 137.0, 136.8, 136.6, 133.8, 133.7, 127.2, 127.1, 124.3, 124.2, 115.7, 115.5, 69.4, 68.9, 34.1, 34.0, 31.2, 31.1, 28.4, 28.2, 28.0, 27.6; *m*/*z* (ESI) 799.3959 (M + Na$^+$; $C_{52}H_{56}NaO_6^+$ requires 799.3975).

7: (14*S*,29*S*)/(14*S*,29*R*) Isomeric Mixture of (1*E*,11*E*,16*E*,26*E*)-3,4:9,10:18,19:24,25-Tetrabenzo-14,29-diphenyl-5,8,20,23-tetraoxatricyclo[25.3.1.1^{12,16}]dotriaconta-1,3,9,11,16,18,24,26-octaene-31,32-dione. Yellow powder; mp 278−279 °C; ν_{max}/cm^{-1} (neat) 1660w (C═O), 1595s (olefinic C═C); δ_H (300 MHz; CF_3COOD) 9.22 and 9.12 (1.00:0.20; 4H, s, CH), 7.66 (8 H, m, Ar), 7.36 (12 H, m, Ar), 7.21 (8 H, m, Ar), 4.78 and 4.73 (8H, s, CH_2), 3.52 and 3.50 (4H, s, CH), 3.19 and 3.17 (8H, s, CH_2); δ_C (75 MHz; CF_3COOD) 185.9, 184.8, 148.7, 148.4, 135.5, 135.2, 133.6, 133.3, 125.0, 124.7, 124.1, 124.0, 122.1 (2C), 119.0 (2C), 117.4, 117.3, 116.7, 116.6, 115.1 (2C), 112.4, 112.2, 103.7, 103.4, 57.3, 56.8, 31.2, 30.1, 25.6, 24.7; *m*/*z* (ESI) 817.3522 (M + H$^+$; $C_{56}H_{49}O_6^+$ requires 817.3580).

8: (1*E*,11*E*,16*E*,26*E*)-3,4:9,10:18,19:24,25-Tetra(6-methoxybenzo)-5,8,20,23-tetraoxatricyclo[25.3.1.1^{12,16}]dotriaconta-1,3,9,11,16,18,24,-26-octaene-31,32-dione. Yellow solid; mp 243−244 °C; ν_{max}/cm^{-1} (neat) 1666w (C═O), 1573m (olefinic C═C); δ_H (300 MHz; $CDCl_3$) 7.95 (4H, s, CH), 7.04 (4H, dd, *J* 8.1 and 7.9, Ar), 6.92 (4H, dd, *J* 7.9 and 1.4, Ar), 6.90 (4H, dd, *J* 8.1 and 1.4, Ar), 4.31 (8H, s, OCH_2), 3.88 (12H, s, OCH_3), 2.82 (8H, m, CH_2), 1.77 (4H, m, CH_2); δ_C (75 MHz, $CDCl_3$) 189.9, 153.0, 148.1, 137.7, 132.6, 131.0, 123.5, 122.6, 113.1, 72.6, 56.2, 29.2, 23.6; *m*/*z* (ESI) 785.3323 (M + H$^+$, 100%; $C_{48}H_{49}O_{10}^+$ requires 785.3320).

9: (1*E*,11*E*,16*E*,26*E*)-3,4:9,10:18,19:24,25-Tetra(6-ethoxybenzo)-5,8,20,23-tetraoxatricyclo[25.3.1.1^{12,16}]dotriaconta-1,3,9,11,16,18,-24,26-octaene-31,32-dione. Yellow solid, mp 262−265 °C; found: C, 74.2; H, 6.5. $C_{52}H_{56}O_{10}$ requires C, 74.3; H, 6.7%; ν_{max}/cm^{-1} (neat) 1665w (C═O), 1572s (olefinic C═C); δ_H (300 MHz; $CDCl_3$) 7.94 (4 H, s, CH), 7.00 (4 H, dd, *J* 8.0 and 7.8, Ar), 6.91 (4 H, dd, *J* 7.8 and 1.4, Ar), 6.88 (4 H, dd, *J* 8.0 and 1.4, Ar), 4.33 (s, 8 H, OCH_2), 4.07 (8 H, q, *J* 7.0, OCH_2CH_3), 2.80 (8 H, m, CH_2), 1.76 (4 H, m, CH_2), 1.43 (12 H, t, *J* 7.0, CH_3); δ_C (100 MHz; $CDCl_3$) 189.8, 152.1, 148.2, 137.7, 132.6, 131.2, 123.3, 122.6, 114.3, 72.4, 64.7, 29.2, 23.5, 15.1; *m*/*z* (ESI) 841.5 (M + H$^+$, 79%).

13: (1*E*,11*E*,16*E*,26*E*)-3,4:9,10:18,19:24,25-Tetrabenzo-14,29-dimethyl-5,8,20,23-tetraoxa-14,29-diazatricyclo[25.3.1.1^{12,16}]dotriaconta-1,3,9,11,16,18,24,26-octaene-31,32-dione. Yellow solid, mp (dec.) 245 °C; ν_{max}/cm^{-1} (neat) 2772w (N—Me), 1668w (C═O), 1596m (olefinic C═C); δ_H (300 MHz; $CDCl_3$) 8.13 (4 H, s, CH), 7.32−7.27 (4 H, m, Ar), 7.21−7.18 (4 H, m, Ar), 6.99−6.94 (4 H, m, Ar), 6.91−6.88 (4 H, m, Ar), 4.46 (8 H, s, OCH_2), 3.71 (8 H, s, CCH_2), 2.36 (6 H, s, CH_3); δ_C (75 MHz; CF_3COOD) 188.2, 187.8, 159.4, 159.3, 145.7, 145.3, 136.1 (2C), 136.1, 132.9, 132.8, 126.9, 126.6, 124.5 (2C), 124.0 (2C), 115.2 (2C), 68.6, 68.3, 57.9, 57.7, 45.1, 44.9; *m*/*z* (ESI) 717.4 (M + Na$^+$, 100%), 1411.5 (2 M + Na$^+$, 87). *m*/*z* (ESI) 695.3133 (M + H$^+$, 100%; $C_{44}H_{43}N_2O_6^+$ requires 695.3116).

14: (1*E*,13*E*,18*E*,30*E*)-3,4:8,9:20,21:28,29-Tetrabenzo-5,10,22,27-tetraoxatricyclo[29.3.1.1^{14,18}]hexatriaconta-1,3,11,13,18,20,28,30-octaene-35,36-dione. Yellow solid; mp 246−247 °C; ν_{max}/cm^{-1} (neat) 1662w (C═O), 1596s (olefinic C═C); δ_H (400 MHz; $CDCl_3$)

8.03 (4 H, s, CH), 7.34−7.31 (4 H, m, Ar), 7.29−7.25 (4 H, m, Ar), 6.95−6.92 (4 H, m, Ar), 6.90−6.87 (4 H, m, Ar), 4.08 (8 H, t, *J* 6.2, OCH_2), 2.87 (8 H, m, CCH_2), 2.06 (8 H, t, *J* 6.0, OCH_2CH_2), 1.77 (4 H, m, CH_2); δ_C (100 MHz; $CDCl_3$) 190.1, 158.1, 136.3, 132.7, 130.7, 130.0, 125.8, 120.1, 111.9, 68.2, 29.4, 25.9, 23.8; *m*/*z* (ESI) 743.3351 (M + Na^+, 100%; $C_{48}H_{48}NaO_6^+$ requires 743.3349).

Crystallography. Crystals suitable for single crystal X-ray diffraction experiments were grown by slow cooling or slow evaporation of solutions of the DEM. Data were collected on a Bruker Kappa Apex CCD diffractometer at 123 K using graphite monochromated Mo Kα radiation ($\lambda = 0.71073$ Å, 0.5° or 1° φ and ω scans as appropriate). Structures were solved by direct methods using the program SHELXS-97and refined by full matrix least-squares refinement on F^2 using the programs SHELXS-97 and SHELXL-97[22] with gui X-Seed.[23] Generally, non-hydrogen atoms of the hosts were refined anisotropically and hydrogen atoms inserted in geometrically determined positions with temperature factors fixed at 1.2 times that of the parent atom. Hydrogen atoms of the hydroxyl groups were located from electron density difference maps and refined. Specific details pertaining to each crystal structure solution and refinement are summarized below.

Crystal Data for 1·2CH₂Cl₂. CCDC deposition number 757267, $(C_{42}H_{36}O_6)_2\cdot(CH_2Cl_2)_4$, $M_r = 1613.12$, triclinic, space group $P\bar{1}$, $a = 14.4827(4)$ Å, $b = 16.0400(4)$ Å, $c = 19.258(1)$ Å, $\alpha = 68.049(1)°$, $\beta = 87.473(1)°$, $\gamma = 68.047(2)°$, $V = 3824.6(2)$ Å^3, $Z = 2$, $D_{calc} = 1.401$ g·cm^{-3}, μ(Mo Kα) = 0.360 mm^{-1}. Of 14274 unique reflections measured, 7160 had $I > 2\sigma(I)$, *R* indices $[I > 2\sigma(I)]$, $R_1 = 0.0719$, $wR_2 = 0.1383$, GoF on $F^2 = 1.017$ for 994 refined parameters and 10 restraints.

Crystal Data for 2·CH₂Cl₂. CCDC deposition number 757268, $C_{46}H_{44}O_{10}\cdot CH_2Cl_2$, $M_r = 841.74$, triclinic, space group $P\bar{1}$, $a = 8.8260(5)$ Å, $b = 13.737(1)$ Å, $c = 18.333(2)$ Å, $\alpha = 69.160(7)°$, $\beta = 80.028(4)°$, $\gamma = 89.354(2)°$, $V = 2042.8(3)$ Å^3, $Z = 2$, $D_{calc} = 1.368$ g·cm^{-3}, μ(Mo Kα) = 0.220 mm^{-1}. Of 9297 unique reflections measured, 2702 had $I > 2\sigma(I)$, *R* indices $[I > 2\sigma(I)]$, $R_1 = 0.0854$, $wR_2 = 0.1487$, GoF on $F^2 = 0.966$ for 536 refined parameters and 0 restraints.

Crystal Data for (*s,s*)-5·C₆H₅Cl. CCDC deposition number 757269, $C_{46}H_{44}O_6\cdot C_6H_5Cl$, $M_r = 805.36$, monoclinic, space group $P2_1/c$, $a = 16.4092(3)$ Å, $b = 16.9899(3)$ Å, $c = 17.0534(4)$ Å, $\beta = 116.98(3)°$, $V = 4237.0(2)$ Å^3, $Z = 4$, $D_{calc} = 1.263$ g·cm^{-3}, μ(Mo Kα) = 0.142 mm^{-1}. Of 10313 unique reflections measured, 5258 had $I > 2\sigma(I)$, *R* indices $[I > 2\sigma(I)]$, $R_1 = 0.0631$, $wR_2 = 0.1157$, GoF on $F^2 = 1.015$ for 545 refined parameters and 0 restraints.

Crystal Data for (*s,s*)-6·1¹/₂*p*-Xylene. CCDC deposition number 757270, $C_{52}H_{56}O_6\cdot(C_8H_{10})_{3/2}$, $M_r = 936.21$, triclinic, space group $P\bar{1}$, $a = 12.4050(4)$ Å, $b = 13.7850(4)$ Å, $c = 16.6000(4)$ Å, $\alpha = 78.930(2)°$, $\beta = 71.360(2)°$, $\gamma = 80.000(2)°$, $V = 2620.4(1)$ Å^3, $Z = 2$, $D_{calc} = 1.187$ g·cm^{-3}, μ(Mo Kα) = 0.074 mm^{-1}. Of 12581 unique reflections measured, 5356 had $I > 2\sigma(I)$, *R* indices $[I > 2\sigma(I)]$, $R_1 = 0.0902$, $wR_2 = 0.2149$, GoF on $F^2 = 1.044$ for 632 refined parameters and 45 restraints.

Crystal Data for 8·2CH₂Cl₂. CCDC deposition number 757271, $C_{48}H_{48}O_{10}\cdot(CH_2Cl_2)_2$, $M_r = 954.72$, monoclinic, space group $P2_1/n$, $a = 7.8629(3)$ Å, $b = 19.818(1)$ Å, $c = 29.592(1)$ Å, $\beta = 92.019(3)°$, $V = 4608.4(3)$ Å^3, $Z = 4$, $D_{calc} = 1.376$ g·cm^{-3}, μ(Mo Kα) = 0.316 mm^{-1}. Of 9432 unique reflections measured, 4889 had $I > 2\sigma(I)$, *R* indices $[I > 2\sigma(I)]$, $R_1 = 0.0615$, $wR_2 = 0.1086$, GoF on $F^2 = 1.016$ for 581 refined parameters and 0 restraints.

Crystal Data for 9. CCDC deposition number 757272, $(C_{52}H_{56}O_{10})_{1/2}$, $M_r = 420.48$, orthorhombic, space group *Pbca*, $a = 16.9103(5)$ Å, $b = 14.9230(4)$ Å, $c = 17.4123(6)$ Å, $V = 4394.0(2)$ Å^3, $Z = 8$, $D_{calc} = 1.271$ g·cm^{-3}, μ(Mo Kα) = 0.087 mm^{-1}. Of 5097 unique reflections measured, 2256 had $I > 2\sigma(I)$, *R* indices $[I > 2\sigma(I)]$, $R_1 = 0.0488$, $wR_2 = 0.0974$, GoF on $F^2 = 0.881$ for 282 refined parameters and 0 restraints.

Crystal Data for 11·¹/₂*p*-Xylene·1¹/₂H₂O. = CCDC deposition number 757273, $C_{46}H_{44}O_7\cdot(C_8H_{10})_{1/2}\cdot(H_2O)_{3/2}$, $M_r = 788.92$, monoclinic, space group $P2_1/c$, $a = 15.7880(3)$ Å, $b = 15.1484(3)$ Å, $c = 17.6179(6)$ Å, $\beta = 98.792(1)°$, $V = 4164.0(2)$ Å^3, $Z = 4$, $D_{calc} = 1.258$ g·cm^{-3}, μ(Mo Kα) = 0.085 mm^{-1}. Of 10142 unique reflections measured, 4331 had $I > 2\sigma(I)$, *R* indices $[I > 2\sigma(I)]$, $R_1 = 0.0896$, $wR_2 = 0.2048$, GoF on $F^2 = 1.031$ for 532 refined parameters and 16 restraints.

Crystal Data for 13·CH₂Cl₂·Toluene. CCDC deposition number 757274, $C_{44}H_{42}O_6N_2\cdot CH_2Cl_2\cdot C_6H_5CH_3$, $M_r = 871.86$, triclinic, space group $P\bar{1}$, $a = 10.816(2)$ Å, $b = 13.601(3)$ Å, $c = 15.868(3)$ Å, $\alpha = 102.67(3)°$, $\beta = 90.47(3)°$, $\gamma = 102.84(3)°$, $V = 2217(1)$ Å^3, $Z = 2$, $D_{calc} = 1.306$ g·cm^{-3}, μ(Mo Kα) = 0.200 mm^{-1}. Of 10598 unique reflections measured, 4923 had $I > 2\sigma(I)$, *R* indices $[I > 2\sigma(I)]$ $R_1 = 0.0661$, $wR_2 = 0.1691$, GoF on $F^2 = 0.988$ for 560 refined parameters and six restraints.

1·2CH₂Cl₂. DEM **1** crystallizes from dichloromethane solution as a 1:2 solvate in the triclinic crystal system and space group $P\bar{1}$. There are two complete DEMs and four solvent molecules in the ASU. One DEM exhibits disorder of the corner aromatic moiety and associated ether flexible linker and is modeled over two positions with site occupancy factors (sof's) of 0.6 and 0.4 for major and minor components. Atoms of both aryl ring components and the minor component of the flexible ether side chain are modeled isotropically, while all other DEM non-hydrogen atoms are allowed to refine anisotropically. Two CH_2Cl_2 solvent molecules are also modeled as disordered: one with three possible positions for the Cl atoms (0.4, 0.3, and 0.3 sof) but a common CH_2 position, and a second over three possible positions (0.5, 0.25, and 0.25) with a common Cl atom position for the 0.25 occupancy components. Temperature factors of disordered non-hydrogen atoms are refined isotropically. Appropriate DFIX restraints are applied to C−C and C−Cl bond lengths of disordered aryl groups and solvent molecules.

2·CH₂Cl₂. DEM **2** crystallizes from dichloromethane solution as a 1:1 solvate in the triclinic crystal system and space group $P\bar{1}$. There are two and a half DEMs and one complete solvent molecule in the ASU. All non-hydrogen atoms are refined anisotropically.

(*s,s*)-5·C₆H₅Cl. The (*s,s*) (with respect to the Me groups of the cyclohexanone moiety) form of DEM **5** crystallizes from chlorobenzene solution as a 1:1 solvate in the monoclinic crystal system and space group $P2_1/c$. There is one complete DEM and one complete (disordered) solvent molecule in the ASU. One DEM methyl group is disordered and modeled over two positions with sof's 0.6 and 0.4. These disordered carbon atoms are refined isotropically as are all carbon atoms of the disordered chlorobenzene solvent, which is rotationally disordered and modeled over three positions, with three orientations for the Cl atom and associated in-plane displacement of the aryl rings. Sof's are fixed at 0.5, 0.3, and 0.2 for the different positions and the aryl rings restrained to be regular hexagons.

(*s,s*)-6·1¹/₂*p*-Xylene. The (*s,s*) (with respect to the *t*-Bu groups of the cyclohexanone moiety) form of DEM **6** crystallizes from *p*-xylene solution as a 1:1.5 solvate in the triclinic crystal system and space group $P\bar{1}$. There is one complete DEM and one and a half xylene molecules in the ASU, with the half xylene molecule centered on special position 0, 0, ¹/₂. Both *t*-Bu-cyclohexyl moieties of the DEM are disordered over two positions, with sof's of 0.7 and 0.3 resulting from rotation of the *t*-Bu group and displacement of carbon atoms 3 and 4 of the cyclohexyl ring. The disorder does not reflect inclusion of (*s,r*)-**6** but instead results from a lesser component of "reverse folded" (*s,s*)-**6**, i.e. with the out-of-plane carbon atoms of the envelope conformer of the *t*-Bu-cyclohexyl group pointing downward with respect to the V of the folded DEM and the *t*-Bu groups pointing upward. The large bulk of the *t*-Bu group means that the space occupied by these two conformers is similar.

8·2CH₂Cl₂. DEM **8** crystallizes from dichloromethane solution as a 1:2 solvate in the monoclinic crystal system and space group $P2_1/n$. There are two and a half DEMs and two complete solvent molecules in the ASU. All non-hydrogen atoms are refined anisotropically.

9. DEM **9** crystallizes nonsolvated from toluene solution in the orthorhombic crystal system and space group *Pbca*. There is a half DEM in the ASU, and all non-hydrogen atoms are refined anisotropically.

11·*p*-Xylene·1¹/₂H₂O. DEM **11** crystallizes as a mixed solvate from wet *p*-xylene solutions in the monoclinic crystal system and space group $P2_1/c$. There is one complete DEM, one and a half water molecules, and two and a half *p*-xylene molecules in the ASU. The *p*-xylene solvent is disordered and two and a half molecules are modeled with aryl rings approximately centered on the special position 0, 0, ¹/₂, resulting in two overlapping positions for the *p*-xylene solvent. The longer of the flexible ether linkers is disordered in one $-CH_2CH_2-$ group, with two equally occupied positions modeled. A water molecule, present at 0.5 occupancy, is associated with one of these positions and is within hydrogen bonding distance of the water molecule that forms a hydrogen bond bridge between the two $C{=}O$ groups. All disordered atoms are refined isotropically while all other non-hydrogen atoms are refined anisotropically. Bond length restraints are applied by use of appropriate DFIX cards to disordered moieties.

$13\cdot CH_2Cl_2\cdot$Toluene. DEM **13** crystallizes as a mixed solvate from dichloromethane/toluene solutions in the triclinic crystal system and space group $P\bar{1}$. There is one complete DEM, one toluene, and one CH_2Cl_2 molecule in the ASU, no disorder is noted, and all non-hydrogen atoms are refined anisotropically.

Acknowledgment. We acknowledge funding from the Australian Research Council (ARC).

Supporting Information Available: Experimental details and characterization data (including NMR spectra and ORTEP diagrams) for all compounds. This material is available free of charge via the Internet at http://pubs.acs.org.

References

(1) Calixarenes, although discovered early in the 20th century, were first described in detail about 30 years ago: Gutsche, C. D.; Muthukrishnan, R. *J. Org. Chem.* **1978**, *43*, 4905–4906. Gutsche, C. D.; Muthukrishnan, R. *Tetrahedron Lett.* **1979**, *24*, 2213–2216. Gutsche, C. D.; Dhawan, B.; No, K. H.; Muthukrishnan, R. *J. Am. Chem. Soc.* **1981**, *103*, 3782–3792. Many reviews describe some of the applications to which calixarenes have been put, including, recently (but by no means comprehensively), enclosing void space: Dalgarno, S. J.; Thallapally, P. K.; Barbour, L. J.; Atwood, J. L. *Chem. Soc. Rev.* **2007**, *36*, 236–245. self assembly into a range of "porous" structures: Coleman, A. W.; Jebors, S.; Shahgaldian, P.; Ananchenko, G. S.; Ripmeester, J. A. *Chem. Commun.* **2008**, 2291–2303. in metal based catalysts: Homden, D. M.; Redshaw, C. *Chem. Rev.* **2008**, *108*, 5086–5130. and preparation of multi-calixarene "daisy chains" Sameni, S.; Jeunesse, C.; Matt, D.; Harrowfield, J. *Chem. Soc. Rev.* **2009**, *38*, 2117–2146.

(2) Resorcinarenes were almost certainly first prepared in the late 19th century: Baeyer, A. *Ber Dtsch. Chem. Ges.* **1872**, *5*, 25. Baeyer, A. *Ber. Dtsch. Chem. Ges.* **1872**, *5*, 280. although it was only in 1968 that the cyclic structure was confirmed: Erdtman, H.; Högberg, S.; Abrahamsson, S.; Nilsson, B. *Tetrahedron Lett.* **1968**, *9*, 1679. These versatile molecules have been comprehensively reviewed: Timmerman, P.; Verboom, W.; Reinhoudt, D. N. *Tetrahedron* **1996**, *52*, 2663.

(3) The first description of these condensation products appeared in 1905: Robinson, G. M. *J. Chem. Soc.* **1915**, *102*, 266. But the correct structures were proposed much later: Oliverio, A.; Boumis, N. *Ann. Chim.* (*Rome*) **1952**, *42*, 168. Garofano, T.; Oliverio, A. *Ann. Chim.* (*Rome*) **1957**, *47*, 896. And verified by crystal structure analysis: Liquori, A. M.; Bertinotti, F.; Carelli, V.; Nardi, A. M. *Ric. Sci., Suppl.* **1952**, *22*, 65. Collet provides a comprehensive review: Collet, A. *Tetrahedron* **1987**, *43*, 5725. And hydrogen bonded networks are covered in: Hardie, M. J. In *Supramolecular Assembly via Hydrogen Bonds II, Book Series: Structure and Bonding*; Mingos, D. M. P., Ed.; Springer-Verlag: Berlin, Heidelberg, New York, 2004; Vol. 111, pp 139−174.

(4) First prepared in 1905: Behrend, R.; Meyer, E.; Rusche, F. *Justus Liebigs Ann. Chem.* **1905**, *339*, 1. and named after their pumpkin shape: Mock, W. L. *Top. Curr. Chem.* **1995**, *175*, 1. Cucurbiturils have been recently reviewed: Lagona, J.; Mukhopadhyay, P.; Chakrabarti, S.; Isaacs, L. *Angew. Chem., Int. Ed.* **2005**, *44*, 4844. These molecules often require functionalization: Lee, J. W.; Samal, S.; Sawapalam, N.; Kim, H. J.; Kim, K. *Acc. Chem. Res.* **2003**, *36*, 621. Kim, K.; Selvapalam, N.; Ko, Y. H.; Park, K. M.; Kim, D.; Kim, J. *Chem. Soc. Rev.* **2007**, *36*, 267.

(5) Crown ethers were first synthesized by Pedersen in the 1960s: Pedersen, C. J. *J. Am. Chem. Soc.* **1967**, *89*, 2495. and by Pedersen, C. J. *J. Am. Chem. Soc.* **1967**, *89*, 7017. And they have been widely used as metal complexing agents and supramolecular tectons ever since. Diverse recent applications include components of supramolecular daisy chains: Cantrill, S. J.; Youn, G. J.; Stoddart, J. F.; Williams, D. J. *J. Org. Chem.* **2001**, *66*, 6857. and "molecular meccano": Cantrill, S. J.; Fulton, D. A.; Heiss, A. M.; Pease, A. R.; Stoddart, J. F.; White, A. J. P.; Williams, D. J. *Chem.—Eur. J.* **2000**, *6*, 2274. while metal complexation by crown ether moieties enables the construction of electroactive polymers: Fabre, B.; Simonet, J. *Coord. Chem. Rev.* **1998**, *178*, 1211. and organic/inorganic hybrid materials: Akutagawa, T.; Endo, D.; Noro, S. I.; Cronin, L.; Nakamura, T. *Coord. Chem. Rev.* **2007**, *251*, 21 amongst many others .

(6) Ronson, T. K.; Hardie, M. J. *CrystEngComm* **2008**, *10*, 1731.

(7) Busi, S.; Saxell, H.; Fröhlich, R.; Rissanen, K. *CrystEngComm* **2008**, *10*, 1803.

(8) Suwinska, K.; Coleman, A. W. *CrystEngComm* **2008**, *10*, 1302.

(9) Shkurenko, O.; Suwinska, K.; Coleman, A. W. *CrystEngComm* **2008**, *10*, 821.

(10) Mastalerz, M.; Rivera, H. J. E.; Hüggenberg, W.; Merz, K.; Oppel, I. M.; Dyker, G. *CrystEngComm* **2008**, *10*, 1120.

(11) Bilge, S.; Coles, S. J.; Davies, D. B.; Hursthouse, M. B.; Krlrç, Z.; Rutherford, J. S.; Shaw, R. A. *CrystEngComm* **2008**, *10*, 873.

(12) Higham, L. T.; Kreher, U. P.; Raston, C. L.; Scott, J. L.; Strauss, C. R. *CrystEngComm*, submitted.

(13) Giarrusso, M. A.; Higham, L. T.; Kreher, U. P.; Mohan, R. S.; Rosamilia, A. E.; Scott, J. L.; Strauss, C. R. *Green Chem.* **2008**, *10*, 842.

(14) Higham, L. T.; Kreher, U. P.; Raston, C. L.; Scott, J. L.; Strauss, C. R. *Org. Lett.* **2004**, *6*, 3257.

(15) Higham, L. T.; Kreher, U. P.; Raston, C. L.; Scott, J. L.; Strauss, C. R. *Org. Lett.* **2004**, *6*, 3261.

(16) Kreher, U. P.; Rosamilia, A. E.; Raston, C. L.; Scott, J. L.; Strauss, C. R. *Org. Lett.* **2003**, *5*, 3107.

(17) Rosamilia, A. E.; Giarrusso, M. A.; Scott, J. L.; Strauss, C. R. *Green Chem.* **2006**, *8*, 1042.

(18) Scott, J. L.; Strauss, C. R. In *Eco-Friendly Processes for the Synthesis of Fine Chemicals*; Ballini, R., Ed.; RSC Publishing: Cambridge, U.K., 2009; pp 220−235.

(19) McKinnon, J. J.; Spackman, M. A.; Mitchell, A. S. *Acta Crystallogr., B* **2004**, *60*, 627.

(20) Takahashi, O.; Yamasaki, K.; Kohno, Y.; Ueda, K.; Suezawa, H.; Nishio, M. *Chem.—Asian J.* **2006**, *1*, 852.

(21) Higham, L. T.; Kreher, U. P.; Mulder, R. J.; Strauss, C. R.; Scott, J. L. *Chem. Commun.* **2004**, 2264.

(22) Sheldrick, G. M. *Acta Crystallogr., A* **2008**, *A64*, 112.

(23) Barbour, L. J. *J. Supramol. Chem.* **2001**, *1*, 189.